Spin Ice: Magnetic Excitations without Monopole Signatures Using Muon Spin Rotation

S. R. Dunsiger,[1,*] A. A. Aczel,[2] C. Arguello,[3] H. Dabkowska,[4] A. Dabkowski,[4] M.-H. Du,[5] T. Goko,[3,6]

B. Javanparast,[7] T. Lin,[7] F. L. Ning,[3,8] H. M. L. Noad,[2] D. J. Singh,[5] T. J. Williams,[2]

Y. J. Uemura,[3,†] M. J. P. Gingras,[7,9,‡] and G. M. Luke[2,9,§]

[1]*Physik Department, Technische Universität München, D-85748 Garching, Germany*
[2]*Department of Physics and Astronomy, McMaster University, Hamilton, Ontario L8S 4M1, Canada*
[3]*Department of Physics, Columbia University, New York, New York 10027, USA*
[4]*Brockhouse Institute for Materials Research, McMaster University, Hamilton, Ontario L8S 4M1, Canada*
[5]*Materials Science and Technology Division, Oak Ridge National Laboratory, Oak Ridge, Tennessee 37831-6114, USA*
[6]*TRIUMF, 4004 Wesbrook Mall, Vancouver, British Columbia, V6T 2A3, Canada*
[7]*Department of Physics and Astronomy, University of Waterloo, Waterloo, Ontario, N2L 3G1, Canada*
[8]*Department of Physics, Zhejiang University, Hangzhou 310027, China*
[9]*Canadian Institute for Advanced Research, Toronto, Ontario M5G 1Z8, Canada*
(Received 4 August 2011; published 11 November 2011)

Theory predicts the low temperature magnetic excitations in spin ices consist of deconfined magnetic charges, or monopoles. A recent transverse-field (TF) muon spin rotation (μSR) experiment [S. T. Bramwell *et al.*, Nature (London) **461**, 956 (2009)] reports results claiming to be consistent with the temperature and magnetic field dependence anticipated for monopole nucleation—the so-called second Wien effect. We demonstrate via a new series of μSR experiments in $Dy_2Ti_2O_7$ that such an effect is not observable in a TF μSR experiment. Rather, as found in many highly frustrated magnetic materials, we observe spin fluctuations which become temperature independent at low temperatures, behavior which dominates over any possible signature of thermally nucleated monopole excitations.

Spin ices, such as $Ho_2Ti_2O_7$ and $Dy_2Ti_2O_7$, are topical highly frustrated magnetic systems which exhibit a gamut of very interesting phenomena [1,2]. In $(Ho/Dy)_2Ti_2O_7$, the Ho^{3+} and Dy^{3+} magnetic ions reside on the vertices of a pyrochlore lattice of corner-sharing tetrahedra. A large single ion anisotropy forces the moment to point strictly along local $\langle 111 \rangle$ crystalline axes, along the line which connects the centers of the two adjoining tetrahedra and their common vertex, making the moments classical "local" Ising spins. Since Ho^{3+} and Dy^{3+} carry a large magnetic moment of $\sim 10\ \mu_B$, the dipolar interaction in these systems is ~ 1 K at nearest neighbor distance and of similar magnitude as the Curie-Weiss temperature θ_{CW} [2]. The frustration in spin ices stems from the $1/r^3$ long-range nature of the magnetic dipolar interaction and its consequential "self-screening" (r is the distance between ions) [3–5]. As a result, spin ices are frustrated ferromagnets with low-energy states characterized by two spins "pointing in" and two spins "pointing out" on each tetrahedron—the 2-in/2-out rule which defines minimum energy spin configurations. These map onto the allowed proton configurations in water ice which obey the Bernal-Fowler ice rules [2], hence the name spin ice.

The dipolar spin ice model [6] and its refinement [7] yield an accurate microscopic quantitative description of the equilibrium thermodynamic properties of spin ices, both in zero and nonzero magnetic field. In contrast, the problem of the dynamical response of the moments in spin

ices remains much less studied and understood. An exciting recent development in that direction is the realization that the "2-in/2-out" spin configurations may be described via a divergence-free coarse-grained magnetization density field [5,8]. A thermal fluctuation causing the flip of an Ising spin from an "in" to an "out" direction amounts to the creation of a nearest-neighbor pair of magnetization source and sink on the two adjoining tetrahedra or, in other words, to the nucleation of "magnetic monopoles" out of the spin-ice-rule obeying vacuum [5]. Particularly interesting is the observation that monopoles in dipolar spin ice interact via an emerging Coulomb potential which decays inversely proportional to the distance which separates them and are therefore deconfined [5]. A recent numerical study [9] provides evidence that the temperature dependence of the relaxation time determined in ac magnetic susceptibility measurements [10] can be rationalized in terms of thermally activated monopoles, at least above 1 K. The wave vector dependence of the neutron scattering intensity suggests power law spin correlations, which are a prerequisite for monopoles with effective Coulomb interactions [11]. Yet, perhaps the reported direct evidence for the presence of monopoles in spin ice and a determination of their effective charge is the most intriguing recent result [12].

In weak electrolytes, including water ice, characterized by a small dissociation rate constant K, the so-called second Wien effect describes the nonlinear increase of K under an applied electric field. In a recent paper [12],

Bramwell and co-workers have drawn further on the analogy between magnetic moments in spin ice and protons in water ice [2]. Using Onsager's accurate theory of the Wien effect [13], Bramwell *et al.* put forward an elegant model to describe the dependence of the monopole nucleation rate $\kappa(T, H)$ in spin ice on temperature T and external applied magnetic field H. They proposed that a measurement of $\kappa(T, H)$ could yield the monopole charge Q. To that effect, the authors of Ref. [12] used μSR in a transverse-field (TF) geometry to determine $\kappa(T, H)$ and extract a value $Q_{exp} \sim 5\mu_B/\text{Å}$, close to the value $Q_{theo} \sim 4.6\mu_B/\text{Å}$ anticipated by theory [5].

In this Letter, we discuss how the weak TF μSR experiment of Ref. [12], as a means to observe the second Wien effect in spin ice, was flawed in its conceptual design and execution and incorrect in its theoretical interpretation of the muon spin depolarization rate. Monte Carlo calculations show that the internal magnetic field at the expected muon locations in $Dy_2Ti_2O_7$ spin ice material is ''large'' (~ 0.3 T) and has a broad distribution, preventing the observation of TF muon precession. We present evidence that the coherent muon precession in weak ($H \sim 1$ mT) TF seen in Ref. [12] originated rather from the sample holder and other parts of the sample environment. In contrast, our zero-field μSR results exhibit low-temperature muon spin relaxation which is temperature independent from 4 K down to 20 mK.

Positive muons provide a pointlike real space magnetic probe averaging over the Brillouin zone, in contrast with magnetization measurements, which measure only the $Q = 0$ response. In a μSR experiment, essentially 100% spin-polarized positive muons are implanted in a material and precess in the local magnetic field $\mathbf{B}(\mathbf{r})$. The muons subsequently decay (with lifetime $\tau_\mu = 2.2$ μs) into a positron (emitted preferentially in the direction of the muon spin at the time of decay) and two undetected neutrinos. An asymmetry signal, obtained from the decay histograms of opposing positron detectors, represents the projection of the muon spin polarization function onto the axis defined by the detectors. Since the muons are created fully spin polarized (via the parity-violating weak decay of their parent pions), μSR experiments may be performed in zero (ZF), longitudinal (LF), or transverse (TF) magnetic field. As in nuclear magnetic resonance (NMR), the depolarization results from both dynamic (T_1) and static (T_2) processes. Further details describing μSR are found elsewhere [14].

TF-μSR—In a TF experiment, an external magnetic field is applied perpendicular to the initial muon spin polarization direction. For arbitrary electronic spin fluctuation rates, an approximate analytic form for the high TF-μSR polarization function is given by a relaxation envelope multiplied by a cosine precession signal [14,15],

$$P_\mu(t) = \exp[-(\Delta^2/\nu^2)(e^{-\nu t} - 1 + \nu t)]\cos(\omega t). \quad (1)$$

In Eq. (1), $\Delta = \gamma_\mu B$ is the muon gyromagnetic ratio times the rms instantaneous internal magnetic field at the muon site B and ν is the field fluctuation rate. In the fast fluctuation ($\nu \gg \Delta$) regime, the envelope becomes $\exp(-\Delta^2 t/\nu)$ whereas, in the slow fluctuation ($\nu \ll \Delta$) regime, the envelope reduces to $\exp(-\Delta^2 t^2/2)$, which is independent of ν. Hence, the relaxation in a transverse field (TF) never takes an exponential form where the relaxation rate $1/T_1 \propto \nu$, as assumed by Bramwell *et al.* [12]. As discussed further below, such behavior is only applicable to ZF and LF measurements. As the fluctuation rate of the electronic moments decreases and a significant spectral density develops near zero frequency, the local field at the muon site becomes the vector sum of the applied and internal fields. As we show, this net field in dipolar spin ice has a much larger rms value than the applied field H. Therefore the muon polarization function is not given by a cosine with a frequency corresponding to the applied field but, instead, is rapidly damped to zero.

From the discussion above, a crucial issue is whether the internal field distribution $P(B(\mathbf{r}))$ in a spin ice has significant weight below the applied external field of $H \sim 1$ mT. As a first step to address this question, we use a loop algorithm [16] in Monte Carlo (MC) simulations of a realistic microscopic model of $Dy_2Ti_2O_7$ [7] to calculate $P(B(\mathbf{r}))$ at the most probable muon locations, as determined by density functional theory (DFT) calculations [17]. We find, confirming naive expectations, that $P(B(\mathbf{r}))$ is heavily populated for fields of several hundreds of millitesla. Such values are consistent with the estimate of ~ 0.5 T obtained by Lago *et al.* from LF-μSR decoupling measurements in $Dy_2Ti_2O_7$ [18]. In fact, for all four lowest energy potential muon stopping sites, we find vanishing $P(B(\mathbf{r}))$ at $|(B(\mathbf{r}))| \to 0$.

Figures 1(a) and 1(b) show TF-μSR spectra measured in single crystals of $Dy_2Ti_2O_7$ mounted using GE varnish on an intrinsic GaAs plate (blue triangles), as well as results
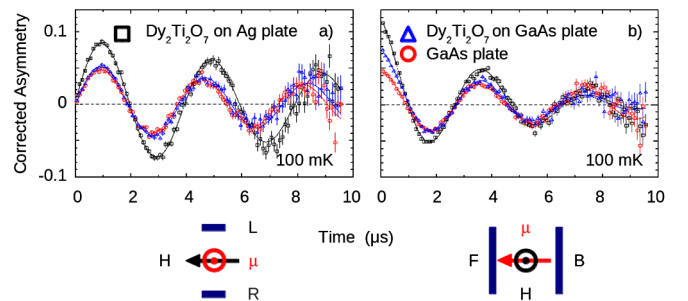

FIG. 1 (color online). TF μSR spectra measured at $T = 100$ mK in $Dy_2Ti_2O_7$ with two different counter geometries. In (a), the applied field $H = 2$ mT lies in the plane of the platelike coaligned mosaic of single crystals. In (b), H is perpendicular to the plates. In both cases H is along the crystallographic [100] direction. The positron detectors are indicated as back (B), forward (F), left (L), and right (R).

on a blank GaAs plate without the $Dy_2Ti_2O_7$ sample (red circles) with an external field of 2 mT in both cases. The crystals were grown using floating zone image furnace methods, with the speed of 4 mm/h. GaAs was chosen as it exhibits no precession at the muon Larmor frequency since all muons form muonium, a hydrogenlike muon-electron bound pair [19]. As a result, the observed red precession signal in Figs. 1(a) and 1(b) is a purely instrumental background from muons which land elsewhere in the dilution refrigerator or in the silver (Ag) sample holder. The signal with the $Dy_2Ti_2O_7$ sample on the GaAs plate (blue) is essentially identical to the background contribution in Fig. 1(a) at long ($t \gtrsim 1$ μs) times. This demonstrates that there is no long-lived muon precession signal originating from the specimen, consistent with the aforementioned expectation based on DFT-MC calculations [17]. The small applied $H = 2$ mT is hence negligible compared to $B(r)$. The small difference in Fig. 1(b) at early times ($t \lesssim 1$ μs) comes from the longitudinal relaxation of the μSR signal in the $Dy_2Ti_2O_7$ sample, visible here because the initial muon spin polarization is parallel to the positron detector axis. This difference is absent in Fig. 1(a) where, due to the chosen experimental geometry, the initial muon polarization is perpendicular to the detector axis. TF-μSR spectra measured with the $Dy_2Ti_2O_7$ crystals mounted on a high purity Ag plate for the same two experimental geometries are shown in black. Using a metal (e.g., silver) backing plate ensures the sample is in good thermal contact. Additionally, silver (taken alone) produces an essentially undamped TF-μSR precession signal. The increased signal amplitude relative to the signal using a GaAs backing reflects the contribution of muons landing in parts of the Ag backing not covered by the sample. Such TF-μSR spectra measured using Ag are essentially identical to those reported in Ref. [12]. Note that in both instances, to account for history dependent effects, care was taken to cool the samples in zero field before applying 2 mT at base temperature and taking data while warming. We note that the evolution of the TF depolarization rate tracks the magnetization [10]. We speculate that a stray field, proportional to the dc magnetization, is generated within the Ag plate in the areas between the crystallites of $Dy_2Ti_2O_7$. Muons landing in such a region undergo slow relaxation due to the inhomogeneous stray field, proportional to the applied field, consistent with observations of Bramwell *et al.* [12].

The above experiments, performed in a dilution refrigerator, require a cold finger sample holder to provide thermal contact to the sample. In contrast, by using a ^{4}He gas-flow cryostat operating at temperatures above $T = 2$ K, one can perform μSR without complications due to a background signal by suspending the specimen on thin tape. The TF-μSR signal observed in such a "background free" apparatus is shown in Fig. 2(a) in $H = 2$ mT. The absence of a precession signal at $T = 2$ K confirms that
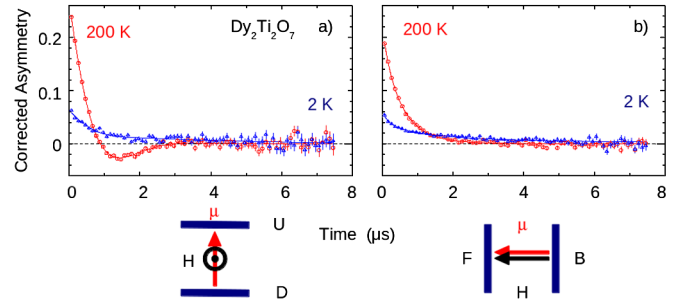

FIG. 2 (color online). Background free (a) TF = 2 mT and (b) ZF μSR spectra measured in $Dy_2Ti_2O_7$. Note the overdamped precession signal in (a). The positron detectors are indicated as back (B), forward (F), up (U), and down (D).

any long lived precession signal seen at $T \lesssim 2$ K does not originate from $Dy_2Ti_2O_7$. Rather, it is a background signal from the sample holder or cryostat. This constitutes the first of our two main results.

ZF-μSR—A more effective method for studying spin dynamics in magnetic systems is to measure the spin polarization in the ZF/LF geometry [14]. At high temperatures, in the fast fluctuation regime, the spin lattice relaxation rate is $1/T_1 = 2\Delta^2/\nu$ in zero applied field [14]. As shown in Fig. 3, $1/T_1$ increases as temperature decreases. This is due to the combined effect of changes in the size of Δ as the Dy^{3+} excited crystal electric field levels are depopulated and the slowing down of the Dy^{3+} fluctuation rate ν. The relaxation rate peaks at $T \approx 50$ K and drops below, entering the slow fluctuation regime, consistent with earlier studies on powder samples [18]. Below $T = 50$ K the muon spin polarization exhibits a two component form, indicating that the local magnetic environment consists of a large quasistatic field [responsible for the rapid loss of polarization seen in Fig. 2(b) at 2 K] coexisting with a fluctuating field component (which gives the damping of
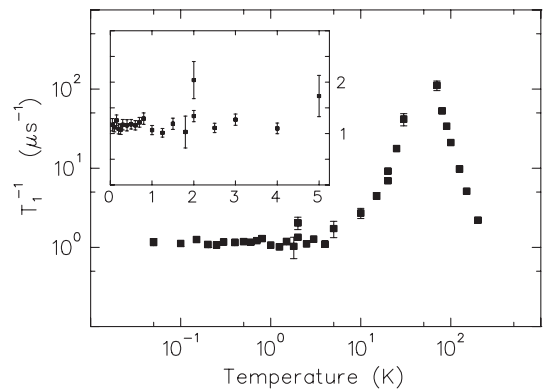

FIG. 3. Muon spin relaxation rate in $Dy_2Ti_2O_7$. Individual μSR spectra were analyzed using a phenomenological stretched exponential form $P_Z(t) \propto \exp(-(t/T_1)^\beta)$ commonly used to model glassy systems. The low temperature behavior of T_1^{-1} is shown on an expanded linear scale in the inset. The exponent β drops monotonically from ~0.75 at 150 K to 0.4 below 5 K.

the remaining polarization). The amplitude of the slowly relaxing component at $T \lesssim 50$ K is 1/3 of the initial polarization, as expected for a cubic material where 1/3 of the muon polarization is on average parallel to $\mathbf{B}(\mathbf{r})$ [14]. Analogous decreases in Dy^{3+} fluctuation rate over 4 orders of magnitude between 300 and 8 K have been observed using zero field ^{47}Ti NQR [20] and nuclear forward scattering [21].

We observe a substantial $1/T_1 \sim 1\ \mu s^{-1}$ relaxation rate at $T \lesssim 5$ K, which is more than an order of magnitude above our detection limit ($\sim 10^{-2}\ \mu s^{-1}$). This observation contrasts dramatically with the activated behavior anticipated for magnetic monopoles [9] and is startling given the highly Ising nature of the Dy^{3+} spins, where large energy barriers against single spin flip processes separate quasidegenerate ice rules states [2]. The origin of this temperature independent relaxation is as yet unclear. We note that so-called persistent spin dynamics have been observed in a wide range of geometrically frustrated materials [22,23]. Oddly, the characteristic rare earth spin fluctuation rates extracted using various techniques differ dramatically in $Dy_2Ti_2O_7$, as do the values when comparing the two isostructural compounds $A_2Ti_2O_7$ (A = Dy, Ho) [10,24–28]. The strong hyperfine interaction between the electronic and nuclear spin species should also not be neglected, particularly in the latter compound, as highlighted by the pronounced Schottky anomaly observed arising from nuclear contributions to the magnetic specific heat [29].

Dy-based compounds form a variety of model Ising systems [30]. However, many of them exhibit unexpected dynamic spin fluctuations at low temperatures: (1) the single molecular magnetic system $[DyPc_2]^0$, characterized by a doubly degenerate ground state and large magnetic anisotropy, exhibits a tunneling regime [31], suggesting such temperature independent behavior is a more pervasive phenomenon [32]; (2) the geometrically frustrated Ising antiferromagnet dysprosium aluminum garnet, where marked changes in the characteristic relaxation times over several orders of magnitude have been reported as a function of applied fields [30]; (3) even the archetypal dilute Ising dipolar ferromagnet dysprosium ethyl sulphate, which exhibits unexpectedly high relaxation rates within the ordered state [33].

Despite a seemingly compelling argument for spin dynamics caused by monopoles [5,9], additional spin relaxation processes dominate the behavior observable using ZF-μSR in $Dy_2Ti_2O_7$ spin ice. In Heisenberg spin systems, geometrical frustration may lead to spin liquid behavior [34] where spin fluctuations persist to absolute zero. Understanding the low temperature dynamics in the Ising $Dy_2Ti_2O_7$ system will require the construction of an effective low energy Hamiltonian containing non-Ising terms [35]. The present work clarifies the nature of static and dynamic contributions to the internal magnetic field as probed using μSR and describes evidence of unusual

spin excitations in a model Ising system. It poses the challenge to comprehensively understand the microscopic mechanism(s) causing the temperature independent muon spin relaxation within the broader context of geometrically frustrated systems [23].

*sarah.dunsiger@frm2.tum.de
†tomo@lorentz.phys.columbia.edu
‡gingras@gandalf.uwaterloo.ca
§luke@mcmaster.ca
[1] M. J. Harris *et al.*, Phys. Rev. Lett. **79**, 2554 (1997).
[2] S. T. Bramwell and M. J. P. Gingras, Science **294**, 1495 (2001).
[3] M. J. P. Gingras and B. C. den Hertog, Can. J. Phys. **79**, 1339 (2001).
[4] S. V. Isakov, R. Moessner, and S. L. Sondhi, Phys. Rev. Lett. **95**, 217201 (2005).
[5] C. Castelnovo *et al.*, Nature (London) **451**, 42 (2008).
[6] B. C. den Hertog and M. J. P. Gingras, Phys. Rev. Lett. **84**, 3430 (2000).
[7] T. Yavors'kii *et al.*, Phys. Rev. Lett. **101**, 037204 (2008).
[8] I. A. Ryzhkin, JETP **101**, 481 (2005).
[9] L. D. C. Jaubert and P. C. W. Holdsworth, Nature Phys. **5**, 258 (2009).
[10] J. Snyder *et al.*, Phys. Rev. B **69**, 064414 (2004).
[11] T. Fennell *et al.*, Science **326**, 415 (2009).
[12] S. T. Bramwell *et al.*, Nature (London) **461**, 956 (2009).
[13] L. Onsager, J. Chem. Phys. **2**, 599 (1934).
[14] Y. J. Uemura, in *Muons in Physics, Chemistry and Materials*, edited by S. L. Lee, R. Cywinski, and S. H. Kilcoyne (Inst. of Phys. Publishing, London, 1999), p. 85.
[15] R. S. Hayano *et al.*, Phys. Rev. B **20**, 850 (1979).
[16] R. G. Melko and M. J. P. Gingras, J. Phys. Condens. Matter **16**, R1277 (2004).
[17] See Supplemental Material at http://link.aps.org/supplemental/10.1103/PhysRevLett.107.207207 for DFT-MC calculations.
[18] J. Lago *et al.*, J. Phys. Condens. Matter **19**, 326210 (2007).
[19] R. F. Kiefl *et al.*, Phys. Rev. B **32**, 530 (1985).
[20] K. Kitagawa *et al.*, Phys. Rev. B **77**, 214403 (2008).
[21] J. P. Sutter *et al.*, Phys. Rev. B **75**, 140402(R) (2007).
[22] Y. J. Uemura *et al.*, Phys. Rev. Lett. **73**, 3306 (1994).
[23] P. A. McClarty *et al.*, J. Phys. Condens. Matter **23**, 164216 (2011).
[24] J. Snyder *et al.*, Nature (London) **413**, 48 (2001).

[25] K. Matasuhira *et al.*, J. Phys. Condens. Matter **13**, L737 (2001).

[26] K. Matsuhira *et al.*, J. Phys. Condens. Matter **12**, L649 (2000).

[27] J. P. Clancy *et al.*, Phys. Rev. B **79**, 014408 (2009).

[28] G. Ehlers *et al.*, J. Phys. Condens. Matter **16**, S635 (2004).

[29] S. T. Bramwell *et al.*, Phys. Rev. Lett. **87**, 047205 (2001).

[30] W. P. Wolf, Braz. J. Phys. **30**, 794 (2000).

[31] F. Branzoli *et al.*, Phys. Rev. B **82**, 134401 (2010).

[32] N. Vernier and G. Bellessa, J. Phys. Condens. Matter **15**, 3417 (2003).

[33] A. H. Cooke *et al.*, Proc. R. Soc. A **306**, 335 (1968).

[34] L. Balents, Nature (London) **464**, 199 (2010).

[35] H. R. Molavian, M. J. P. Gingras, and B. Canals, Phys. Rev. Lett. **98**, 157204 (2007).